Subinertial variability in the deep ocean near the East Pacific Rise between 9° and 10°N

Xinfeng Liang[1] and Andreas M. Thurnherr[1]

Received 5 January 2011; revised 16 February 2011; accepted 1 March 2011; published 25 March 2011.

[1] The subinertial variability of deep-ocean currents near the crest of the East Pacific Rise in the tropical East Pacific is examined using observations from a collection of moored instruments augmented with sea-surface height data. The moored velocity observations reveal low-frequency currents with characteristic time scales of 1–3 months and maximum speeds up to 10 cm/s. Directly over the ridge axis, the subinertial motions are dominated by the along-axial (meridional) velocities, which are coherent in phase and amplitude along the entire length of the ridge segment between 9°and 10°N. With increasing distance from the ridge crest the low-frequency currents become weaker and less dominated by the along-axial flow component. Lag-correlations between the velocity records indicate westward signal propagation with a speed on the same order as the speed of westward-propagating sea-surface height anomalies, which are also associated with characteristic time scales of 1–3 months. As, furthermore, the subinertial velocities at depth are significantly correlated with geostrophic near-surface currents estimated from sea-surface height data, we conclude that the subinertial velocity field near the EPR crest is mainly a superposition of velocities associated with eddies propagating westward across the ridge and "topographic flows", such as trapped waves and boundary currents. **Citation:** Liang, X., and A. M. Thurnherr (2011), Subinertial variability in the deep ocean near the East Pacific Rise between 9° and 10°N, *Geophys. Res. Lett.*, *38*, L06606, doi:10.1029/2011GL046675.

1. Introduction

[2] Subinertial variability of the velocity field is ubiquitous around the world ocean and is mainly dominated by the intraseasonal frequency band (20–150 days) [e.g., *Stammer*, 1997]. Since subinertial variability plays an important role in dispersing mass, heat and other ocean tracers, gaining a better understanding of it is essential for investigating ocean circulation and marine biogeochemistry. In the eastern tropical Pacific, subinertial variability in the upper ocean has been revealed by satellite and in situ data [e.g., *Miller et al.*, 1985; *Perigaud*, 1990; *Giese et al.*, 1994; *Farrar and Weller*, 2006; *Willett et al.*, 2006]. This variability is particularly pronounced in two latitude bands: one is at 5°–7°N and is dominated by tropical instability waves, the other is centered at 10°–12°N and is dominated by anticyclonic eddies [e.g., *Giese et al.*, 1994]. Using in situ and satellite data *Farrar and Weller* [2006] show that both wave- and eddy-like motions contribute to the observed subinertial variability near 10°N. Due to a lack of in situ data from the deep ocean, most previous work has focused on signals near the sea-surface, that is, the subinertial variability in the deep eastern tropical Pacific has not yet been intensively studied.

[3] The presence of the East Pacific Rise (EPR) adds complexity to the dynamics of the subinertial variability in the eastern tropical Pacific Ocean. *Palacios and Bograd* [2005] suggest that, due to the conservation of potential vorticity, the EPR can affect the intensity and propagation of westward-propagating Tehuantepec and Papagayo eddies. Elsewhere, observations near other mid-ocean ridges have revealed topographic effects on the ocean dynamics. For example, *Thomson et al.* [1990] show that the bottom-intensification of subinertial flows observed over the Juan de Fuca Ridge are related to the ridge topography.

[4] For this study, we analyze a velocity data set from current meters and McLane Moored Profilers deployed close to the crest of the EPR segment between 9°and 10°N (section 2) and relate the velocity observations to sea-surface height data in order to examine whether the subinertial variability observed in the upper ocean affects the deep eastern tropical Pacific (section 3). In section 4, the observations are discussed.

2. Data and Methods

[5] During a project called LADDER (LArval Dispersal along the Deep East-pacific Rise), five current-meter moorings were deployed near the crest of EPR between 9° and 10°N in November 2006 and recovered in November 2007 (Figure 1). The array consists of two flank moorings (EF and WF) and three axial moorings (NA, CA and SA). Each mooring was equipped with an Aanderaa RCM-11 current meter recording velocities at 2450 m with a sample interval of 20 minutes. These current meters on the axial and flank moorings recorded velocities about 100 m and 500 m above the seabed, respectively. Additional velocity observations at 2450 m were made by two moorings equipped with McLane Moored Profilers (MMP) deployed on the western flank of the EPR (W1 and W3 in Figure 1). Each MMP collected about three velocity samples at 2450 m per day. Due to ballasting problems the MMP records are shorter than the current-meter records (W1: November 2006–August 2007; W3: November 2006–October 2007). For additional information about the observations, refer to *Thurnherr et al.* [2011].

[6] To examine the relationship between the upper- and deep-ocean variability, we also used the multi-mission gridded sea-surface height anomaly (SSHA) data set from AVISO. The horizontal resolution of the gridded SSHA data is 1/3° × 1/3° and the sample interval is 1 day. SSHA data

[1]Lamont-Doherty Earth Observatory, Earth Institute at Columbia University, Palisades, New York, USA.

0094-8276/11/2011GL046675

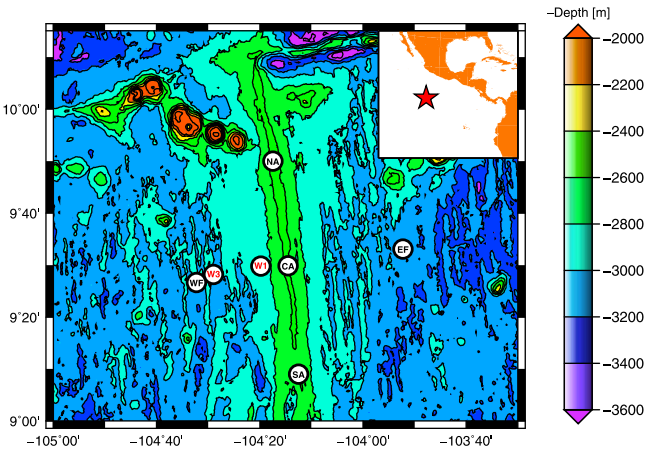

Figure 1. Topography of the EPR segment between 9° and 10°N. Locations of current meter moorings and McLane Moored Profilers are labeled with circles. Names of stations are marked in the circles (current meter moorings: black; MMPs: red). The red star in the inset shows the location of the study region.

are available for the entire sampling period of the LADDER mooring array.

[7] In order to investigate the subinertial variability, all velocity and SSHA data were low-pass filtered with a fourth-order Butterworth filter with a cut-off frequency of 0.05 cycles/day. Rotary spectra of velocities were calculated using the method of *Mooers* [1973]. To determine the propagation of the subinertial variability, lag-correlations of the vector currents were calculated using the simple regression method of *Hanson et al.* [1992].

3. Results

[8] Low-pass filtered velocities recorded by the current meters and MMPs at 2450 m reveal subinertial variability with characteristic time scales of one to three months (Figure 2). Along the ridge crest, the low-frequency currents from the three axial moorings (NA, CA and SA) are coherent in both phase and amplitude (Figure 2a, top). Maximum currents at the axial stations are about 10 cm/s and the ratio of the rms cross-axial (zonal) to along-axial (meridional) velocities is about 1/2 in all three records. In the cross-axial direction (Figure 2a, bottom), the low-frequency currents from CA and W1 are highly correlated, as are the velocities from W3 and WF. In contrast, there is little apparent coherence between the low-frequency currents recorded at EF/CA and at W1/W3, respectively. The meridional coherence scale (>70 km based on the distance between NA and SA) is larger than the zonal coherence scale (<20 km based on the distance between W1 and W3). The amplitude of the meridional velocities is decreasing with increasing distance from the ridge crest, while the ratio of the rms zonal to meridional velocity is increasing from 1/2 at CA to about 1 at EF and WF.

[9] To examine the frequency composition of the subinertial variability, rotary spectra of the current-meter velocities were calculated. Both the anticyclonic and cyclonic components of the spectra show energetic peaks with periods between 20 and 100 days. Comparison of the anticyclonic and cyclonic components from different moorings indicates that the cyclonic subinertial energy is similar in all records ($2.8(\pm1.3) \times 10^{-2}$ m^2 s^{-2}) while the anticyclonic energy is similar at WF and EF ($1.3(\pm0.1) \times 10^{-2}$ m^2 s^{-2}) but stronger (and similar) at CA, NA and SA ($7.1(\pm2.4) \times 10^{-2}$ m^2 s^{-2}). This implies that, over the ridge axis, the anticyclonic subinertial energy is amplified by a factor of 5–6.

[10] In order to investigate the relationship between the upper- and deep-ocean variability, we first examined the temporal and spatial characteristics of the subinertial variability at the sea-surface. Longitude-time and latitude-time plots of subinertial SSHA along 9.5°N and 104.5°W (Figure 3a) indicate westward signal propagation with a speed of about 15 cm/s whereas there is no clear meridional propagation. The characteristic period of the variability at the sea surface is about one to three months, the same as the dominant low-frequency variability in our mooring observations. In the time-latitude plot of SSHA (Figure 3a, right) a band of intense variability appears between 10° and 15°N. According to *Giese et al.* [1994] the subinertial variability

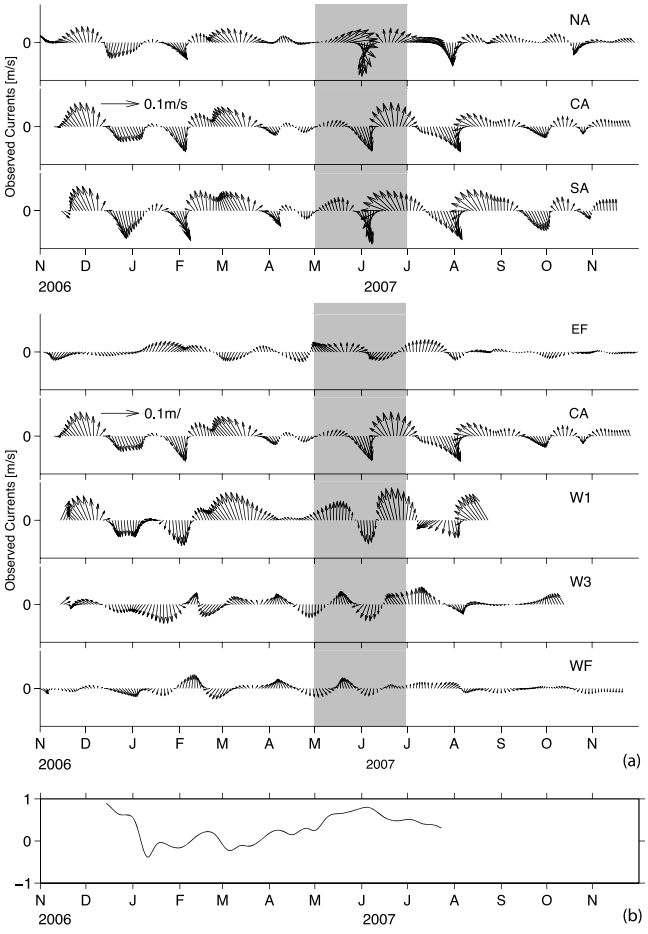

Figure 2. (a) Low-pass filtered velocities (north upward) recorded by the current meters and MMPs at 2450 m. (top) Velocities from the stations along the ridge crest; (bottom) velocities from the stations across the ridge crest. Shaded regions show the period when two anticyclonic eddies passed the observation site directly (see Figure 3). (b) Correlation of the meridional velocities between W1 and W3 calculated with overlapping two months segments. All labels are at the beginning of the months.

in this latitude band is dominated by anticyclonic eddies. While the cores of these eddies crossed the EPR north of our observation site (9°–10°N), they nevertheless dominate the surface variability there.

[11] The similarity of the dominant subinertial time scales suggests that the deep-ocean subinertial variability is related to the westward-propagating SSHA signals shown in Figure 3a. To determine the propagation of the deep-ocean variability, we calculated lag-correlations between the velocity records of neighboring moorings. The results indicate consistently westward signal propagation at 9.5°N with speeds that are on the same order, although consistently smaller, than the SSHA propagation speeds (Figure 3b).

[12] We further compared the geostrophic currents estimated from SSHA gradient data near NA to the subinertial currents recorded by the current meter at NA (Figure 4). The comparison shows low-frequency variation of the correlations between the upper- and deep-ocean subinertial variability of both the zonal and meridional velocity components. Large negative correlations occurred in both zonal and meridional velocities between May and July 2007, when two

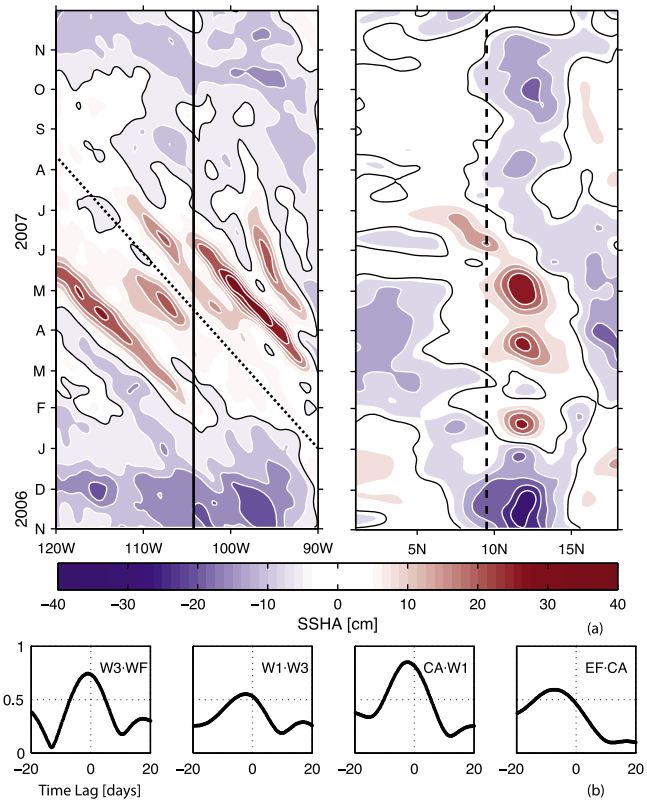

Figure 3. (a) (left) Time-longitude plot of subinertial SSHA at 9.5°N. The solid line shows the longitude of the ridge crest and the doted line indicates a westward speed of 15 cm/s; (right) time-latitude plot of subinertial SSHA at 104.5°W. The dashed line shows the latitude where the geographic center of the observation is located (9.5°N). All labels are at the beginning of the months. (b) Lag-correlations of low-frequency currents at 2450 m between adjacent stations in the cross-axial direction. Negative lags imply westward propagation and the speeds for the four panels (from right to left) are 7 cm/s, 6 cm/s, 10 cm/s and 8 cm/s, respectively.

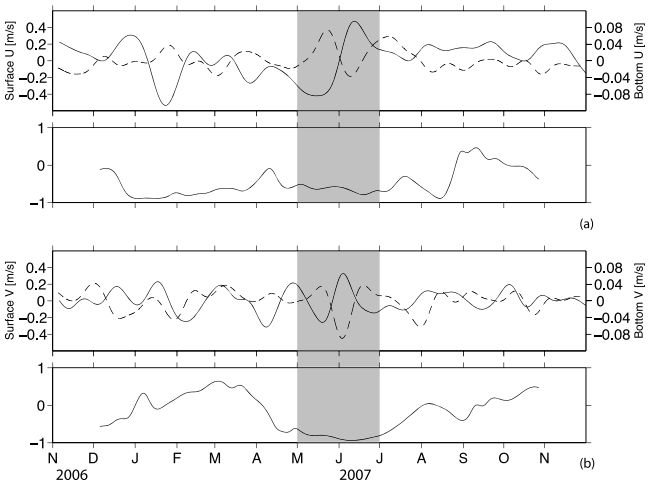

Figure 4. (a) (top) Zonal velocities of geostrophic currents (solid) estimated from the SSHA data near NA and observed deep-ocean currents (dash) at NA; (bottom) their correlation calculated with overlapping two months segments. (b) (top) Meridional velocities of geostrophic currents (solid) and observed deep-ocean currents (dash) at NA are shown; (bottom) their correlation calculated with overlapping two months segments. Shaded regions show the period during which two energetic anticyclonic eddies affected the observation site. The estimated geostrophic currents and the observed deep-ocean currents are plotted with an offset of 8 days. The correlation is also calculated with an offset of 8 days. All labels are at the beginning of the months.

energetic anticyclonic eddies affected the observation site. Here the current meter record is lagged by 8 days, which is the optimal time lag resulting from the lag correlation between the altimetry-derived geostrophic currents of low-temporal resolution and observed deep-ocean currents of high-temporal resolution. The accuracy of the optimal time lag was investigated and verified by repeating the time lagging of the time series between May and July 2007 using low-pass filters with different cut-off frequencies.

4. Discussion

[13] Away from topography, subinertial velocity variability in the ocean is typically dominated by low vertical modes [e.g., *Wunsch*, 1997]. Near mid-ocean ridges, the dynamics are expected to be complicated by topographic effects, such as (standing or propagating) topographic waves [e.g., *Allen and Thomson*, 1993] and topographic deformation of eddies [e.g., *Adams and Flierl*, 2010]. In spite of this expectation, our observations indicate that the subinertial zonal velocities near the EPR crest in the eastern tropical Pacific are anticorrelated with the near-surface velocities most of the time, consistent with dominance of the first baroclinic mode. While the correlation between the corresponding meridional velocities is much more variable in time, strong anticorrelation is apparent between May and July 2007, when SSHA data show two eddies passing over the ridge crest near the observation site.

[14] The subinertial variability in our moored velocity data is associated with a larger meridional (along the EPR axis) than zonal (across the EPR axis) coherence scale.

We interpret this observation as a result of topographic effects on the dynamics. For example, *Allen and Thomson* [1993] show that, for ridge with an approximately triangular cross section, like the EPR in our study region, the along-axial velocity will decay to almost zero within a distance of one internal deformation radius R from the ridge crest. Using the vertical scale h = 500 m corresponding to the height of the steep inner flanks of the EPR crest in this region, the observed buoyancy frequency near the ridge crest $N = 8 \times 10^{-4}$ s^{-1}, as well as the Coriolis parameter $f = 2.5 \times 10^{-5}$ s^{-1}, the internal deformation radius $R = \frac{Nh}{f} \approx$ 16 km. Alternatively both the difference between the cross- and along-axial coherence scales and the dominance of the meridional velocities near the ridge axis are also consistent with the model of *Adams and Flierl* [2010], which shows that when eddies in the deep ocean approach the ridge crest, they will be elongated along the ridge and therefore induce strong meridional velocities near the crest of meridionally trending ridges. Additional support for our inference of strong topographic effects on the regional dynamics is provided by the observation that the anticyclonically polarized subinertial motion directly over the ridge crest is amplified by a factor of 5 or so. We interpret this amplification as a consequence of the conservation of potential vorticity resulting from "vortex squashing" associated with motion across the ridge crest.

[15] Our observations indicate westward propagation of the subinertial variability in our study region both at the sea surface and near the depth of the ridge crest. While similar in magnitude, the propagation speed at depth is consistently smaller than the propagation speed at the surface. The persistent 7-month-long anticorrelation between the subinertial zonal velocities at depth and at the surface strongly suggests that any difference in zonal propagation speed must be localized as, otherwise, the velocities at the surface and at depth would be expected to decorrelate quickly. This inference is consistent with the model of *Adams and Flierl* [2010], which predicts that the upper layers of baroclinic eddies passing a ridge crest barely "feel" the topography whereas the velocities at depth can be substantially affected, resulting in a significant slowdown in the cross-ridge propagation speed. In a recent paper, based on results from a 2-dimensional regional circulation model, *McGillicuddy et al.* [2010] interpret the low-frequency variation of the meridional currents over the EPR crest in this region as the consequence of back-and-forth sweeping of north- and southward boundary currents that flow along the western and eastern ridge flanks, respectively. Our results suggest that this back-and-forth sweeping is likely caused by deep-reaching eddies propagating across the ridge axis. In addition to eddies, our data also suggest a likely influence of the North Equatorial Counter Current (NECC) [e.g., *Kessler*, 2006] on the circulation in this region. In particular, we interpret the eastward geostrophic flow inferred from SSH data between August and October 2007 as a likely signature of the NECC. While we cannot preclude the possibility that the NECC affected our velocity measurements near the ridge crest, we see no strong evidence for such an effect.

[16] In conclusion, we interpret the subinertial variability of the observed velocity field close to the EPR crest in the tropical East Pacific to be mainly the result of a superposition of velocities associated with eddies propagating westward across the ridge and "topographic flows", such as the trapped waves discussed by *Allen and Thomson* [1993] and the boundary currents described by *McGillicuddy et al.* [2010]. This implies that the eddies apparent in sea surface height not only dominate the subinertial velocity variability in the upper ocean but also exert strong influence on the deep ocean, even near mid-ocean ridges, where topographic effects complicate the dynamics. Considering the ubiquitousness of eddies in the ocean we expect that the circulation near other portions of the global mid-ocean ridge system is similarly dominated by mesoscale variability and topographic effects. This is particularly important for dispersal of larvae and geochemical tracers associated with hydrothermal sources that are found primarily along the crest of mid-ocean ridges.

[17] **Acknowledgments.** Co-funding of the LADDER project by the biological and physical oceanography divisions of the National Science Foundation under grant 0425361 is gratefully acknowledged.

[18] The Editor thanks Emilio Beier and an anonymous reviewer for their assistance in evaluating this paper.

References

Adams, D., and G. Flierl (2010), Modeled interactions of mesoscale eddies with the East Pacific Rise: Implications for larval dispersal, *Deep Sea Res., Part I*, *57*(10), 1163–1176.

Allen, S., and R. Thomson (1993), Bottom-trapped subinertial motions over midocean ridges in a stratified rotating fluid, *J. Phys. Oceanogr.*, *23*(3), 566–581.

Farrar, J. T., and R. A. Weller (2006), Intraseasonal variability near 10°N in the eastern tropical Pacific Ocean, *J. Geophys. Res.*, *111*, C05015, doi:10.1029/2005JC002989.

Giese, B., J. Carton, and L. Holl (1994), Sea level variability in the eastern tropical Pacific as observed by TOPEX and Tropical Ocean-Global Atmosphere Tropical Atmosphere-Ocean Experiment, *J. Geophys. Res.*, *99*(C12), 24,739–24,748.

Hanson, B., K. Klink, K. Matsuura, S. Robeson, and C. Willmott (1992), Vector correlation: Review, exposition, and geographic application, *Ann. Assoc. Am. Geogr.*, *82*(1), 103–116.

Kessler, W. (2006), The circulation of the eastern tropical Pacific: A review, *Prog. Oceanogr.*, *69*(2–4), 181–217.

McGillicuddy, D., J. Lavelle, A. Thurnherr, V. Kosnyrev, and L. Mullineaux (2010), Larval dispersion along an axially symmetric mid-ocean ridge, *Deep Sea Res., Part I*, *57*(7), 880–892.

Miller, L., D. Watts, and M. Wimbush (1985), Oscillations of dynamic topography in the eastern equatorial Pacific, *J. Phys. Oceanogr.*, *15*(12), 1759–1770.

Mooers, C. (1973), A technique for the cross spectrum analysis of pairs of complex-valued time series, with emphasis on properties of polarized components and rotational invariants, *Deep Sea Res. Oceanogr. Abstr.*, *20*(12), 1129–1141.

Palacios, D. M., and S. J. Bograd (2005), A census of Tehuantepec and Papagayo eddies in the northeastern tropical Pacific, *Geophys. Res. Lett.*, *32*, L23606, doi:10.1029/2005GL024324.

Perigaud, C. (1990), Sea level oscillations observed with Geosat along the two shear fronts of the Pacific North Equatorial Countercurrent, *J. Geophys. Res.*, *95*(C5), 7239–7248.

Stammer, D. (1997), Global characteristics of ocean variability estimated from regional TOPEX/POSEIDON altimeter measurements, *J. Phys. Oceanogr.*, *27*(8), 1743–1769.

Thomson, R., S. Roth, and J. Dymond (1990), Near-inertial motions over a mid-ocean ridge: Effects of topography and hydrothermal plumes, *J. Geophys. Res.*, *95*(C5), 7261–7278.

Thurnherr, A. M., J. Ledwell, J. Lavelle, and L. Mullineaux (2011), Regional circulation near the crest of the East Pacific Rise between 9° and 10°N, *Deep Sea Res., Part I*, in press.

Willett, C., R. Leben, and M. Lavín (2006), Eddies and tropical instability waves in the eastern tropical Pacific: A review, *Prog. Oceanogr.*, *69*(2–4), 218–238.

Wunsch, C. (1997), The vertical partition of oceanic horizontal kinetic energy, *J. Phys. Oceanogr.*, *27*(8), 1770–1794.

X. Liang and A. M. Thurnherr, Division of Ocean and Climate Physics, Lamont-Doherty Earth Observatory, Earth Institute at Columbia University, 61 Rte. 9W, Palisades, NY 10964, USA. (xliang@ldeo.columbia.edu)